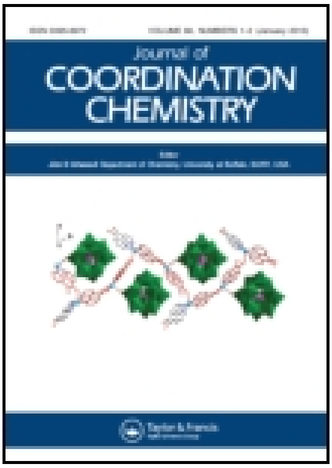

Journal of Coordination Chemistry
Publication details, including instructions for authors and subscription information:
http://www.tandfonline.com/loi/gcoo20

Effect of solvent on the construction of Co(II) coordination polymers containing a semi-rigid bis(benzimidazole) derivative: syntheses, structures, and properties

Xiuli Wang[a], Chunhua Gong[a], Naili Chen[a], Guocheng Liu[a], Hongyan Lin[a] & Jian Luan[a]
[a] Department of Chemistry, Liaoning Province Silicon Materials Engineering Technology Research Centre, Bohai University, Jinzhou, PR China
Accepted author version posted online: 16 Sep 2014.Published online: 13 Oct 2014.

To cite this article: Xiuli Wang, Chunhua Gong, Naili Chen, Guocheng Liu, Hongyan Lin & Jian Luan (2014) Effect of solvent on the construction of Co(II) coordination polymers containing a semi-rigid bis(benzimidazole) derivative: syntheses, structures, and properties, Journal of Coordination Chemistry, 67:21, 3473-3483, DOI: 10.1080/00958972.2014.966100

To link to this article: http://dx.doi.org/10.1080/00958972.2014.966100

Journal of Coordination Chemistry, 2014
Vol. 67, No. 21, 3473–3483, http://dx.doi.org/10.1080/00958972.2014.966100

Effect of solvent on the construction of Co(II) coordination polymers containing a semi-rigid bis(benzimidazole) derivative: syntheses, structures, and properties

XIULI WANG*, CHUNHUA GONG, NAILI CHEN, GUOCHENG LIU, HONGYAN LIN and JIAN LUAN

Department of Chemistry, Liaoning Province Silicon Materials Engineering Technology Research Centre, Bohai University, Jinzhou, PR China

(*Received 2 January 2014; accepted 28 July 2014*)

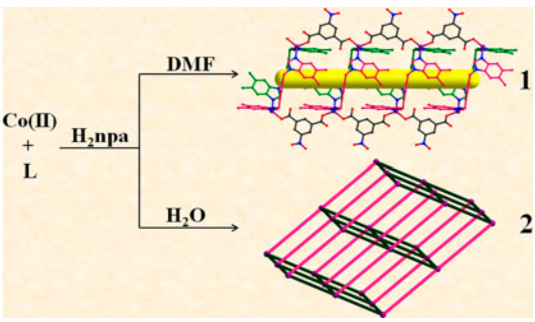

Two Co(II) coordination polymers, [CoL(npa)]·$2H_2O$ (**1**) and [CoL$(Hnpa)_2$] (**2**) (L = 1,4-bis(5,6-dimethylbenzimidazole-1-yl)benzene, H_2npa = 5-nitroisophthalic acid), have been synthesized in different solvent systems and characterized by Infrared (IR) spectroscopy, elemental analysis, and powder and single crystal X-ray diffraction. Compound **1** was synthesized under solvothermal conditions with DMF as solvent and had a pair of L ligands adopting a μ_2-bridging mode and connecting two Co^{2+} cations to generate a 26-membered Co_2L_2 loop. The npa^{2-} link adjacent Co_2L_2 loops via a bis(monodentate) bridging mode to create a 1-D channel-like chain structure. Compound **2** was obtained under hydrothermal conditions, and the carboxylate of the monodeprotonated $Hnpa^-$ adopt a μ_1-$\eta^0:\eta^1$ coordination to connect adjacent Co^{2+} cations into a 2-D polymeric layer. The μ_2-bridging L ligands connect adjacent 2-D $[Co(Hnpa)]_n$ polymeric layers into a 3-D NaCl-like framework. The Co^{2+} cations and the L ligands in compounds **1** and **2** exhibit different coordination geometries and conformations. Effects of solvents on the construction of Co(II) coordination polymers were investigated. In addition, the electrochemical behavior of carbon paste electrodes containing **1** and **2** and the thermal stabilities of **1** and **2** were investigated.

Keywords: Cobalt coordination polymers; Bis(benzimidazole) derivative; 5-Nitroisophthalic acid; Solvent effect; Electrochemical property

*Corresponding author. Email: wangxiuli@bhu.edu.cn

1. Introduction

Design and construction of metal-organic coordination polymers (CPs) have been studied for intriguing architectures and topologies [1], potential applications in luminescence [2], electrochemistry [3], and gas storage [4]. Various effective strategies for synthesis of CPs, such as tuning inorganic anions [5], organic ligands [6], pH values [7], templates and solvent effects [8], as well as hydrothermal [9], *in situ* [10], and ionothermal syntheses [11], have been well documented. Currently, much effort has been devoted to understand the significant role of solvent on the assemblies, structures, and properties of coordination systems [12–15]. The solvent effect has become a vital subject, not only due to the fact that the solvent system is an important parameter in the synthesis of phase-pure crystalline materials and one of the key factors in construction of various coordination networks, but also owing to the possibility of exploring the underlying structure–property correlation resulting from solvent interaction with the host networks [16, 17].

Flexible and rigid bis(benzimidazole) derivatives, as one class of important multidentate N donor ligands, have been widely employed in transition metal complex systems and their coordination behaviors have been investigated by Liu, Ma, Hou, Bu, and our group [18–22]. However, reports on transition metal coordination polymers derived from semi-rigid bis (benzimidazole) derivatives are relatively limited [23–25]. As a continuing effort we selected a semi-rigid bis(benzimidazole) derivative 1,4-bis(5,6-dimethylbenzimidazole-1-yl)benzene (L) as the main ligand and 5-nitroisophthalic acid (H_2npa) as the secondary ligand to react with a Co(II) salt in different solvent systems in order to investigate the effect of different solvents on the construction and structures of the target complexes. As a result, two new metal-organic coordination polymers, [CoL(npa)]·$2H_2O$ (**1**) and [CoL(Hnpa)$_2$] (**2**), have been obtained under solvothermal and hydrothermal conditions, respectively. The effect of solvents on the dimensionality and structures is discussed. The electrochemical behaviors of carbon paste electrodes containing **1** and **2** (**1**–CPE and **2**–CPE, respectively) were studied.

2. Experimental

2.1. *Materials and general methods*

All chemicals for syntheses were purchased from commercial sources and were used as received. L was prepared according to a literature method [26]. The water content of $CoCl_2·6H_2O$ was confirmed by IR and Thermogravimetric (TG) measurement (figure S1, see online supplemental material at http://dx.doi.org/10.1080/00958972.2014.966100). C, H, and N elemental analyses were carried out on a Perkin-Elmer 240C elemental analyzer. IR spectra were obtained on a Varian FT-IR 640 spectrometer with KBr pellets from 400 to 4000 cm^{-1}. Powder X-ray diffraction (PXRD) investigations were carried out with an Ultima IV with D/teX Ultra diffractometer at 40 kV, 40 mA with Cu Kα (λ = 1.5406 Å) radiation. TG data for **1** and **2** were collected on a Pyris Diamond thermal analyzer. A CHI 440 electrochemical workstation connected to a Digital-586 personal computer was used for control of the electrochemical measurements and for data collection. A conventional three-electrode cell was used at room temperature. Carbon paste electrodes containing **1** and **2** were used as the working electrodes. An SCE and a platinum wire were used as reference and auxiliary electrodes, respectively.

2.2. *Preparation of 1 and 2*

2.2.1. [CoL(npa)]·2H_2O (1). A mixture of $CoCl_2·6H_2O$ (0.048 g, 0.2 mM), L (0.040 g, 0.1 mM), H_2npa (0.042 g, 0.2 mM), DMF (8 mL), and NaOH (0.016 g, 0.4 mM) was placed in a 25 mL Teflon reactor. The mixture was heated at 150 °C for four days, then the autoclave was gradually cooled to room temperature. Blue block-shaped crystals (0.019 g, 28% yield based on L) suitable for X-ray diffraction (XRD) were isolated. Elem. Anal. for $C_{34}H_{33}CoN_5O_8$. Calcd (%): C, 58.45; H, 4.73; N, 10.03. Found: C, 58.13; H, 4.64; N, 10.16. IR (KBr, cm^{-1}): 3436w, 2923w, 1624s, 1514m, 1451m, 1366s, 1117s, 619s.

2.2.2. [CoL(Hnpa)$_2$] (2). Compound **2** was prepared in the same way as **1** except that H_2O was used as solvent instead of DMF. Pink block-shaped crystals (0.015 g, 17% yield based on L) suitable for XRD were obtained. Elem. Anal. for $C_{42}H_{34}CoN_6O_{12}$. Calcd (%): C, 57.73; H, 3.90; N, 9.62. Found: C, 57.82; H, 3.82; N, 9.68. IR (KBr, cm^{-1}): 2924w, 1654s, 1536s, 1372m, 1347s, 1119s, 731s.

2.3. *Preparation of carbon paste electrodes containing 1 and 2 (1–CPE and 2–CPE)*

Carbon paste electrodes containing **1** and **2** were fabricated by the following steps. Graphite powder (0.50 g) and **1** or **2** (0.03 g) were ground together with an agate mortar and pestle for approximately 30 min to achieve an even, dry mixture. Then 0.16 mL paraffin oil was added and the mixture was stirred with a glass rod [27]. The homogenized mixture was packed into a 3 mm inner diameter glass tube and a copper wire was added as the electrical contact. The surface of the modified electrodes was polished on a piece of weighing paper to achieve a mirror finish before use.

2.4. *X-ray crystallographic study*

Crystallographic data for **1** and **2** were collected on a Bruker SMART APEX II diffractometer equipped with a CCD area detector and graphite-monochromated Mo Kα (λ = 0.71073 Å) radiation in the ω and θ scan modes. The crystal structures were solved by direct methods using *SHELXS* of the *SHELXTL* crystallographic software package and refined by full-matrix least-squares on F^2 using *SHELXTL* [28]. Non-hydrogen atoms were refined with anisotropic temperature parameters. The disordered O2W in **1** was refined over two sites in a ratio of 45 : 55. The hydrogens of the organic ligands were generated geometrically and refined isotropically. Hydrogen of carboxylic acid group in **2** could not be found from the residual peaks. One H was added on each $Hnpa^-$ anion in **2** to balance the charge, although it is probably disordered over the other H-acceptors in **2** and directly included in the final molecular formula [29]. The crystal, data collection, and refinement parameters for **1** and **2** are summarized in table 1. Selected bond lengths and angles are given in table S1.

3. Results and discussion

3.1. *Description of crystal structures of 1 and 2*

3.1.1. [CoL(npa)]·2H_2O (1). Single crystal X-ray crystallography reveals that **1** is a 1-D structure. As shown in figure 1, **1** consists of one Co(II), one L, one npa^{2-}, and two waters

Table 1. Crystal, data collection, and refinement parameters for **1** and **2**.

	1	**2**
Formula wt.	698.58	873.67
Crystal system	Monoclinic	Monoclinic
Space group	$P2_1/c$	$P2_1/c$
T (K)	296(2)	296(2)
a (Å)	9.579(2)	11.162(8)
b (Å)	27.056(5)	16.428(1)
c (Å)	13.167(2)	10.583(7)
α (°)	90	90
β (°)	100.392(4)	95.614(1)
γ (°)	90	90
V (Å^3)	3356.5(1)	1931.4(2)
Z	4	2
D_{Calcd} (Mg/m^3)	1.382	1.499
μ/(mm^{-1})	0.570	0.520
F (000)	1452	898
R_{int}	0.0762	0.0259
$R_1{}^a$ [$I > 2\sigma(I)$]	0.0736	0.0364
$wR_2{}^b$ (all data)	0.0603	0.0946
GOF	1.009	1.000
$\Delta\rho_{max}$ (e Å^{-3})	1.020	0.470
$\Delta\rho_{min}$ (e Å^{-3})	−0.608	−0.393

$^aR_1 = \Sigma||F_o| - |F_c||/\Sigma|F_o|$.
$^bwR_2 = \Sigma[w(F_o{}^2 - F_c{}^2)^2]/\Sigma[w(F_o{}^2)^2]^{1/2}$.

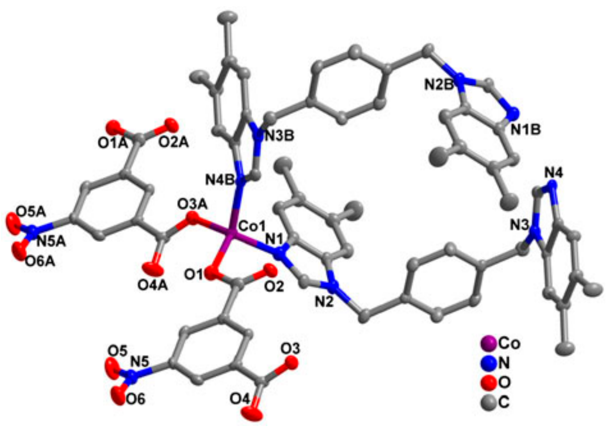

Figure 1. Structure of **1** with 30% probability thermal ellipsoids. The hydrogens and the crystalline water molecules are omitted for clarity (A: −1 + x, y, z; B: 1 − x, 1 − y, 1 − z).

of crystallization. Co1 is in four-coordinate by two O of two carboxylate groups from two npa^{2-} anions [Co1–O1 = 1.952(5) Å, Co1–O3(A) = 1.959(5) Å] and two nitrogens from two L [Co1–N1 = 2.008(6) Å, Co1–N4(B) = 2.033(6) Å], showing a CoN_2O_2 tetrahedral coordination geometry. The bond distances are near those reported for [Co(DNBA)$_2$(pbdmbm)] [30] (pbdmbm = 1,1′-(1,3-propanediyl)bis(5,6-dimethylbenzimidazole), HDNBA = 3,5-dinitrobenzoic acid) with Co–O = 1.955(2) Å and Co–N = 2.037(6) Å.

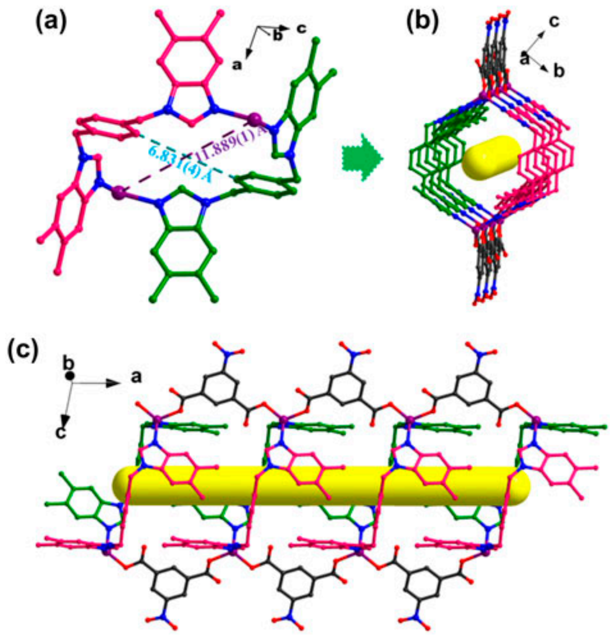

Figure 2. (a) View of the 26-membered $Co_2(L)_2$ loop. The values are the Co–Co and C24–C24 cross-loop distances; (b) view of the 1-D channel along the *a* axis; and (c) view of the 1-D channel along the *b* axis.

In **1**, a pair of L ligands adopts a μ_2-bridging mode, coordinating to two Co^{2+} cations to generate a 26-membered Co_2L_2 loop with dimensions of 6.831(4) × 11.889(1) Å [figure 2(a)]. Adjacent Co_2L_2 loops are further linked by pairs of npa^{2-} anions with a bis(monodentate) bridging mode to create a 1-D channel-like structure [figure 2(b)]. As shown in figure 2(c), the Co(II) are linked by npa^{2-} to form a linear $[Co(npa)]_n$ chain extending along the *a* axis. Luo *et al.* have reported a Zn(II) coordination polymer, $[Zn(L^1)(npa)$

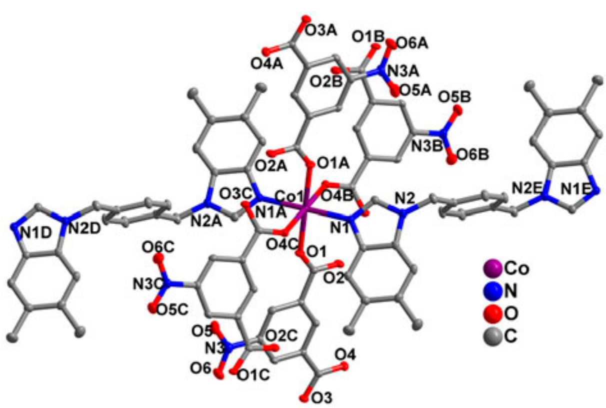

Figure 3. Structure of **2** with 30% probability thermal ellipsoids. The hydrogens are omitted for clarity (A: −*x*, −*y*, 1 − *z*; B: −*x*, −0.5 + *y*, 1.5 − *z*; C: *x*, 0.5 − *y*, −0.5 + *z*; D: −1 + *x*, *y*, −1 + *z*; E: 1 − *x*, −*y*, 1 − *z*).

$(DMF)_{0.5}(H_2O)_{0.5}]_n$ (L^1 = N^4,$N^{4'}$-di(pyridin-4-yl)biphenyl-4,4′-dicarboxamide) [31], that shows a 3-D structure with a 1-D hexagonal channel. The structural differences between the two complexes may be due to the influence of N-donor ligand and metal.

3.1.2. [CoL(Hnpa)$_2$] (2). Single crystal X-ray crystallography reveals that **2** is a 3-D framework. As shown in figure 3, **2** consists of one Co(II), one L, and two $Hnpa^-$. Co1 is in six-coordinate by four oxygens of four carboxylate groups from four $Hnpa^-$ anions [Co1–O1 = 2.109(1) Å, Co1–O1(A) = 2.109(1) Å, Co1–O4(B) = 2.111(1) Å, Co1–O4(C) = 2.111(1) Å] and two benzimidazole nitrogens from two L ligands [Co1–N1 = 2.144(2) Å, Co1–N1(A) = 2.144(2) Å]. These distances are comparable to those in the similar [Co(pbbm)(npa)]·H_2O [32] (pbbm = 1,1-(1,3-propanediyl)bis-1H-benzimidazole), with Co–O = 2.391(4) Å and Co–N = 2.146(2) Å and a CoN_2O_4 octahedral coordination geometry.

In **2**, $Hnpa^-$ anions also adopt a bis(monodentate) bridging mode. Every Co^{2+} cation is linked by four $Hnpa^-$ anions, constructing a 4,4-connected 2-D $[Co\text{-}Hnpa]_n$ layer [figure 4(a)]. The dimensions of the $[Co_4(Hnpa)_4]$ window, as given by the cross-diagonal Co–Co distances, are 10.583(7) × 16.428(1) Å. The μ_2-bridging L connects the Co1 ions, resulting in a 1-D $(CoL)_n$ linear chain [figure 4(b)]. The 1-D linear chains connect with the 2-D polymeric layers through shared Co(II) ions to form a 3-D framework, as shown in figure 4(c).

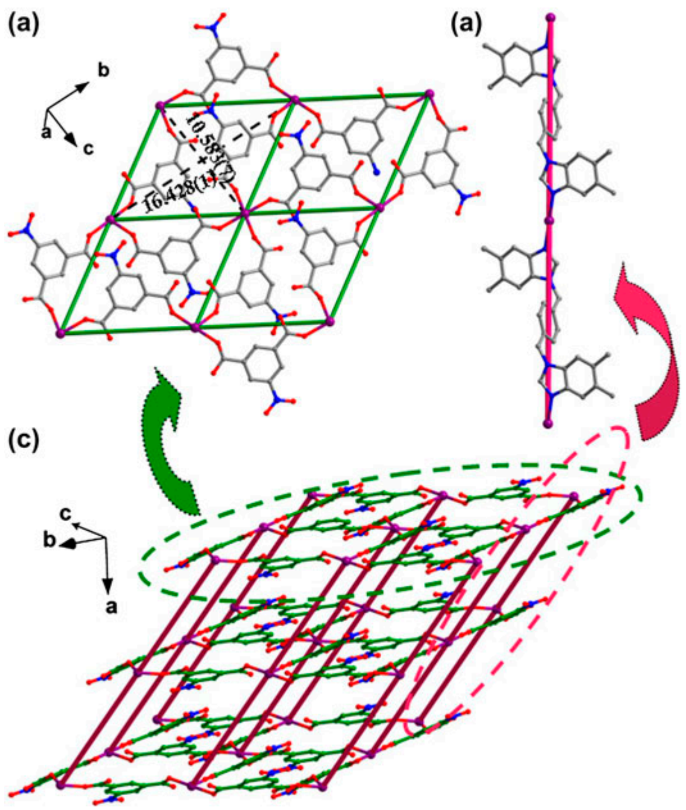

Figure 4. (a) View of the $[Co(Hnpa)_2]$ layer and the Co–Co distances of the $[Co_4\text{-}Hnpa_4]$ window; (b) view of the $[CoL]_n$ chain; and (c) view of the 3-D NaCl-like architecture.

Topologically, the Co(II) ions in the metal-carboxylate layer are viewed as nodes and $Hnpa^-$ as a two-connected linker. Thus each Co-carboxylate layer in **2** can be simplified as a ($4^4 \cdot 6^2$) net-shaped SBU. As the L ligands can also be viewed as two-connected linkers, connecting with the 2-D layer, the whole framework forms a six-connected NaCl-like network with the point symbol of ($4^{12} \cdot 6^3$).

In our recent work, we reported a mixed ligand, Co(II) coordination polymer $\{[Co(L)(npht)] \cdot H_2O\}_n$ (H_2npht = 3-nitrophthalic acid) synthesized under hydrothermal conditions [33], in which the Co(II) ions are five-coordinate in a distorted pyramid coordination geometry by two N of the L ligands and three O from two $npht^{2-}$ ligands, a coordination geometry which is different from that in **2**. In addition, the L ligands exhibited both *syn* and *anti* conformations to link the binuclear $[Co(npht)]_2$ units into a 3-D $CdSO_4$-like framework. In **2**, the L ligands only adopted an *anti* bridging conformation to link the 2-D $[Co(Hnpa)]_n$ polymeric layers through shared Co(II) ions into a 3-D NaCl-like framework. The structural differences between the two complexes may be due to the different stereochemistries of the dicarboxylates.

3.2. *Role of solvents in self-assembly process and various structures*

By employing different solvents (DMF and H_2O) with the same reactants under similar reaction conditions, two different compounds (**1** and **2**) were synthesized, although the basic coordination modes of all the ligands were the same. When DMF was used as a solvent in the synthesis of **1**, Co(II) is four-coordinate with a regular tetrahedral coordination geometry, with the L ligands linking two Co(II) ions into a dinuclear Co_2L_2 loop and the npa^{2-} connecting the adjacent Co_2L_2 loops to form a 1-D channel-like double chain. The L exhibits an *anti* conformation with an intraligand N⋯N (N1–N4) distance between the terminal dimethylbenzimidazole groups of 9.822(2) Å and dihedral angles between the benzimidazole and benzene rings of 80.72° and 83.33° (chart 1). When H_2O is used in the synthesis of **2**, Co(II) is six-coordinate with regular octahedral coordination geometry. The carboxylate groups of $Hnpa^-$ connect adjacent Co(II) ions into 2-D polymeric layers, which are extended by L to create a 3-D NaCl-like framework. The L ligands also have an *anti* conformation, with intraligand N⋯N (N1–N1A) distance between the terminal 5,6-dimethylbenzimidazole groups of 11.251(0) Å, and the dihedral angles between the benzimidazole and benzene rings 83.25° and 85.41°. The structural diversity of **1** and **2** can be attributed to the different solvent systems.

To investigate this solvent-dependent synthesis further, we have attempted to synthesize a compound using a mixed H_2O and DMF solvent system in various ratios (1 : 1, 1 : 2, 2 : 1, and 3 : 8 V : V). However, only **1** was obtained. In addition, solvent mixtures of CH_3OH or THF with H_2O were tested, however, only some irregular small crystals of unknown composition were isolated. Our results indicate that the solvents play an important role in the construction and structure of the compounds. Li *et al.* have reported two Mn^{II}-supramolecular isomers based on different solvent systems (H_2O and DMF), $[Mn_2(pbt)_2(H_2O)_2 \cdot 2H_2O]_n$ (**3**) and $[Mn_2(pbt)_2(H_2O)_2 \cdot DMF]_n$ (**4**) (H_2pbt = 5′-(pyridin-2-yl)-2H,4′H-3,3′-bis(1,2,4-triazole)) [34]. When only H_2O was used, **3**, which exhibits a (3,4)-connected 3-D framework, was obtained. However, when a 1 : 1 (v : v) DMF–H_2O mixed solvent was used, **4**, a rare 3-D **lvt** architecture was obtained. Xiao *et al.* have also reported two Co(II)-based complexes obtained in H_2O, methanol, and DMF, $\{[Co_4(oba)_4(1,4\text{-bix})_4] \cdot 6H_2O\}_n$ (**5**) and $\{[Co_6(oba)_6(1,4\text{-bix})_6] \cdot 2H_2oba \cdot 3\text{-}DMF \cdot 11H_2O\}_n$ (**6**) (H_2oba = 4,4′-oxybis (benzoic acid), 1,4-bix = 1,4-bis(imidazol-l-yl-methyl)benzene) [35]. When a 1 : 1 (v : v) DMF–H_2O mixed

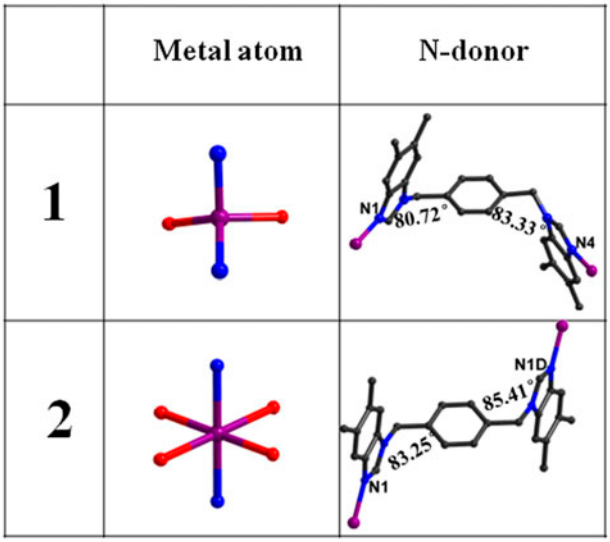

Chart 1. Coordination geometries of Co(II) and conformations of L in **1** and **2**. The values are the dihedral angles between the benzimidazole and benzene rings (D: $1-x$, $-y$, $2-z$).

solvent was used, **5**, a doubly interpenetrated double-layered framework structure was formed. However, when a 1 : 2 DMF : methanol solvent system was used, **6** with a 1-D chain structure was obtained. The structural diversity may be due to the different size and the solubilizing ability of the solvent molecules.

3.3. *IR spectra of 1 and 2*

IR spectra of **1** and **2** are shown in figure S2. The main features of the spectra concern the carboxylate groups of npa^{2-} and Hnpa^{-} and the N-heterocyclic rings of L. In **1**, there is no strong absorption peak around 1700 cm^{-1} for the –COOH stretch, implying that the carboxylate groups in **1** are completely deprotonated [36, 37]. The peaks at 1624 and 1451 cm^{-1} for **1** and 1654 and 1372 cm^{-1} for **2** can be considered as vibrations of the carboxylate groups. The strong peaks at 1514, 1366, 1117, and 619 cm^{-1} for **1** and 1536, 1347, 1119, and 731 cm^{-1} for **2** can be assigned to the vibrations of the benzimidazolyl rings in L [38]. The presence of bands at 2923 cm^{-1} for **1** and 2924 cm^{-1} for **2** can be considered as $\nu_{C\text{-}H}$ stretching frequency of the $–CH_3$ or $–CH_2–$ groups of L.

3.4. *PXRD of 1 and 2*

The powder and simulated XRD patterns of **1** and **2** are depicted in figure S3. The measured PXRD patterns are in agreement with the patterns simulated from the X-ray single crystal data, indicating phase purity of the samples. The difference in reflection intensities between the simulated and the experimental patterns is due to the different orientation of the crystals in the powder samples [39, 40].

3.5. *Thermal stability of 1 and 2*

TG analyses between room temperature and 800 °C under N_2 showed high thermal stability for **1** and **2**, as shown in figure 5. The TG curve of **1** exhibits two obvious weight loss steps. The first of 5.21 wt% from 88 to 106 °C is assigned to elimination of water (Calcd 5.16 wt%). The second weight loss commenced at 318 °C. A residual final weight of 10.64 wt% at 521 °C is consistent with that for CoO (Calcd 10.90 wt%), corresponding to decomposition of the organic components. The TG curve of **2** only shows one weight loss step, corresponding to loss of $Hnpa^-$ and L. The overall framework of **2** begins to collapse at 338 °C and ends at 662 °C, with a residue of 8.21 wt%, consistent with that for CoO (Calcd 8.61 wt%).

3.6. *Electrochemical behaviors of 1–CPE and 2–CPE*

1 and **2** are insoluble in water and in common organic solvents. Thus, carbon paste electrodes modified with **1** and **2** (**1**–CPE and **2**–CPE) were fabricated as working electrodes, the optimal choice to study the electrochemical properties of these complexes [41].

Figures 6 and S5 show the cyclic voltammograms for **1**–CPE and **2**–CPE in a 0.01 M H_2SO_4 + 0.5 M Na_2SO_4 aqueous solution at different scan rates. A reversible redox peak can be seen clearly in the potential range of +750 to –300 mV for **1**–CPE and +950 to −100 mV for **2**–CPE, which could be attributed to a Co(II)/Co(III) redox couple [42]. The mean peak potentials $E_{1/2} = (E_{pa} + E_{pc})/2$ are +232 mV (120 mV s^{-1}) for **1**–CPE and +247 mV (120 mV s^{-1}) for **2**–CPE. With scan rates varying from 40 to 500 mV s^{-1}, the peak potentials changed gradually; the cathodic peak potentials shifted in the negative direction and the corresponding anodic peak potentials shifted in the positive direction with increasing scan rates. The peak currents were proportional to the scan rates (figure S4 and inset of figure S5), which indicated that the redox processes of **1**–CPE and **2**–CPE were surface-controlled.

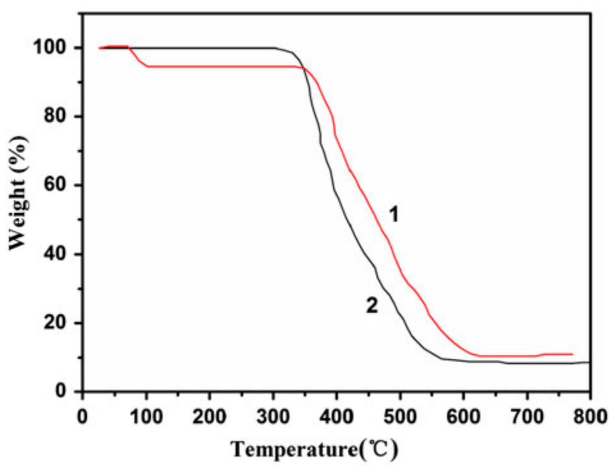

Figure 5. The TG curves of **1** and **2**.

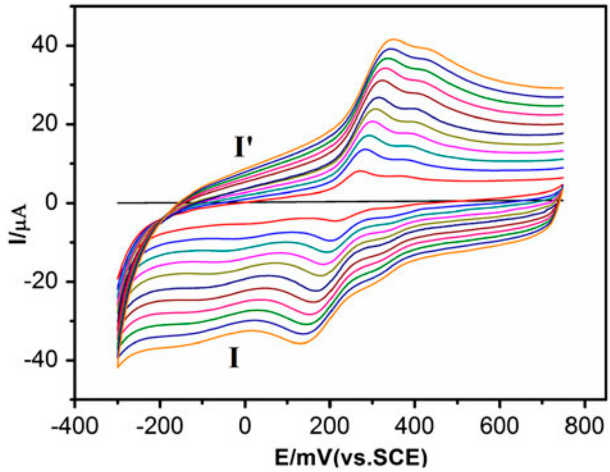

Figure 6. Cyclic voltammograms of **1**–CPE in a 0.01 M H_2SO_4 + 0.5 M Na_2SO_4 aqueous solution in the potential range of 750 to −300 mV at different scan rates (from inner to outer: 40, 80, 120, 160, 200, 250, 300, 350, 400, 450, 500 mV s^{-1}).

4. Conclusion

We obtained two new Co(II) coordination polymers based on 1,4-bis(5,6-dimethylbenzimidazole-1-yl)benzene and 5-nitroisophthalic acid under different solvent systems. Compound **1** has a 1-D channel-like chain and **2** exhibits a 3-D NaCl-like framework. The Co(II) ions and the N-donor ligands in the title complexes exhibit different coordination characteristics and conformations. The structural differences indicate that solvent systems play an important role in the structures of these complexes. This work, to some extent, provides a good example of design and controllable assembly of coordination polymers by reasonable selection of solvent systems.

Supplementary material

Tables of selected bond distances and angles for **1** and **2**; figures of the IR spectrum and TG curves of the $CoCl_2·6H_2O$ starting material, and IR spectra and experimental and simulated PXRD patterns for **1** and **2**; plots of the cathodic peak and anodic peak currents *versus* scan rates for **1**–CPE; cyclic voltammogram for **2**-CPE. CCDC 956793 for **1** and 956792 for **2** contain the supplementary crystallographic data for this article. These data can be obtained free of charge from the Cambridge Crystallographic Data Center via www.ccdc.cam.ac.uk/data_request/cif.

Funding

This work was financially supported by the National Natural Science Foundation of China [grant number 21171025]; Program of New Century Excellent Talents in University (NCET-09-0853); Program of Innovative Research Team in University of Liaoning Province (LT2012020).

References

[1] D.P. Martin, R.M. Supkowski, R.L. Laduca. *Inorg. Chem.*, **46**, 7917 (2007).
[2] F. Luo, Y.X. Che, J.M. Zheng. *Cryst. Growth Des.*, **8**, 2006 (2008).
[3] J.K. Beattie, C.U. Beck, P.A. Lay, A.F. Masters. *Inorg. Chem.*, **42**, 8366 (2003).
[4] L.Y. Du, W.J. Shi, L. Hou, Y.Y. Wang, Q.Z. Shi, Z.H. Zhu. *Inorg. Chem.*, **52**, 14018 (2013).
[5] L. Duan, Y. Ding, X. Meng, W. Li, H. Hou, Y. Fan. *J. Mol. Struct.*, **53**, 975 (2010).
[6] N.A.F. Al-Rawashdeh, S. Chatterjee, J.A. Krause, W.B. Connick. *Inorg. Chem.*, **53**, 294 (2014).
[7] L.F. Ma, L.Y. Wang, D.H. Lu, S.R. Batten, J.G. Wang. *Cryst. Growth Des.*, **9**, 1741 (2009).
[8] T. Devic, C. Serre, N. Audebrand, J. Marrot, G. Férey. *J. Am. Chem. Soc.*, **127**, 12788 (2005).
[9] Z. Chen, D.L. Gao, C.H. Diao, Y. Liu, J. Ren, J. Chen, B. Zhao, W. Shi, P. Cheng. *Cryst. Growth Des.*, **12**, 1201 (2012).
[10] P. Cui, Z. Chen, D.L. Gao, B. Zhao, W. Shi, P. Cheng. *Cryst. Growth Des.*, **10**, 4370 (2010).
[11] Q.Y. Liu, Y.L. Wang, N. Zhang, Y.L. Jiang, J.J. Wei, F. Luo. *Cryst. Growth Des.*, **11**, 3717 (2011).
[12] B. Liu, H. Miao, L.Y. Pang, L. Hou, Y.Y. Wang. *CrystEngComm*, **14**, 2954 (2012).
[13] G.H. Xu, X.Y. He, J.Y. Lv, Z.G. Zhou, Z.Y. Du, Y.R. Xie. *Cryst. Growth Des.*, **12**, 3619 (2012).
[14] M.J. Manos, E.J. Kyprianidou, G.S. Papaefstathiou, A.J. Tasiopoulos. *Inorg. Chem.*, **51**, 6308 (2012).
[15] B. Liu, L.Y. Pang, L. Hou, Y.Y. Wang, Y. Zhang, Q.Z. Shi. *CrystEngComm*, **14**, 6246 (2012).
[16] Q.H. Chen, F.L. Jiang, L. Chen, M. Yang, M.C. Hong. *Chem. Eur. J.*, **18**, 9117 (2012).
[17] C.P. Li, M. Du. *Chem. Commun.*, **47**, 5958 (2011).
[18] Q.X. Liu, Q. Wei, X.J. Zhao, H. Wang, S.J. Li, X.G. Wang. *Dalton Trans.*, **42**, 5902 (2013).
[19] H.Y. Liu, H. Wu, J. Yang, Y.Y. Liu, B. Liu, Y.Y. Liu, J.F. Ma. *Cryst Growth Des.*, **11**, 2920 (2011).
[20] C.Y. Xu, L.K. Li, Y.P. Wang, Q.Q. Guo, X.J. Wang, H.W. Hou, Y.T. Fan. *Cryst. Growth Des.*, **11**, 4667 (2011).
[21] Z.X. Li, Y. Xu, Y. Zuo, L. Li, Q.H. Pan, T.L. Hu, X.H. Bu. *Cryst. Growth Des.*, **9**, 3904 (2009).
[22] X.L. Wang, J.X. Zhang, G.C. Liu, H.Y. Lin, Y.Q. Chen, Z.H. Kang. *Inorg. Chim. Acta*, **368**, 207 (2011).
[23] C.Y. Xu, Q.Q. Guo, X.J. Wang, H.W. Hou, Y.T. Fan. *Cryst. Growth Des.*, **11**, 1869 (2011).
[24] S.K. Chawla. *Polyhedron*, **18**, 1397 (1999).
[25] H.W. Kuai, X.C. Cheng, X.H. Zhu. *J. Coord. Chem.*, **66**, 1795 (2013).
[26] C.B. Aakeröy, J. Desper, B. Leonard, J.F. Urbina. *Cryst. Growth Des.*, **5**, 3865 (2005).
[27] H.Y. Lin, H.L. Hu, X.L. Wang, B. Mu, J. Li. *J. Coord. Chem.*, **63**, 1295 (2010).
[28] G.M. Sheldrick. *Acta Cryst. A*, **64**, 112 (2008).
[29] V. Chandrasekhar, P. Bag, W. Kroener, K. Gieb, P. Müller. *Inorg. Chem.*, **52**, 13078 (2013).
[30] X.L. Wang, S. Yang, G.C. Liu, L.L. Hou, H.Y. Lin, A.X. Tian. *Transition Met. Chem.*, **36**, 891 (2011).
[31] F. Luo, M.S. Wang, M.B. Luo, G.M. Sun, Y.M. Song, P.X. Li, G.C. Guo. *Chem. Commun.*, **48**, 5989 (2012).
[32] X.L. Wang, J.X. Zhang, L.L. Hou, G.C. Liu, H.Y. Lin, J.W. Zhang. *Russ. J. Inorg. Chem.*, **57**, 700 (2012).
[33] G.C. Liu, J.J. Huang, J.W. Zhang, X.L. Wang, H.Y. Lin. *Transition Met. Chem.*, **38**, 359 (2013).
[34] W.W. Dong, D.S. Li, J. Zhao, L.F. Ma, Y.P. Wu, Y.P. Duan. *CrystEngComm*, **15**, 5412 (2013).
[35] B.F. Huang, H.P. Xiao, H. Huang, X.H. Li, J.G. Wang, A. Morsali. *J. Coord. Chem.*, **66**, 904 (2013).
[36] X.J. Gu, D.F. Xue. *Cryst. Growth Des.*, **6**, 2551 (2006).
[37] L.J. Bellamy. *The Infrared Spectra of Complex Molecules*, Wiley, New York (1958).
[38] S.L. Xiao, L. Qin, C.H. He, X. Du, G.H. Cui. *J. Inorg. Organomet. Polym.*, **23**, 771 (2013).
[39] X. Zhou, P. Liu, W.H. Huang, M. Kang, Y.Y. Wang, Q.Z. Shi. *CrystEngComm*, **15**, 8125 (2013).
[40] W. Zhang, L.J. Hao. *J. Coord. Chem.*, **66**, 2110 (2013).
[41] A.X. Tian, J. Ying, J. Peng, J.Q. Sha, H.J. Pang, P.P. Zhang, Y. Chen, M. Zhu, Z.M. Su. *Cryst. Growth Des.*, **8**, 3717 (2008).
[42] T.V. Mitkina, N.F. Zakharchuk, D.Y. Naumov, O.A. Gerasko, D. Fenske, V.P. Fedin. *Inorg. Chem.*, **47**, 6748 (2008).